Ring Formation in Linear Stepwise Polymerization†

Richard J. Rolando‡ and Christopher W. Macosko*

Department of Chemical Engineering and Materials Science, University of Minnesota, Minneapolis, Minnesota 55455. *Received January 28, 1987*

ABSTRACT: We have found the formation of small rings in stepwise polymerization of a vinyl-end-capped bifunctional poly(dimethylsiloxane) (PDMS) and 2-, 3-, and 4-functional siloxanes. Low molecular weight reactants (approximately 200) were used to enhance ring formation. We have shown the number of rings increases in dilute solutions and with equimolar concentrations of reactants. The amount of each lower molecular weight species in the product distribution was determined by gas chromatography (GC) and actual identification of the products was performed by nuclear magnetic resonance (NMR) and mass spectroscopy–gas chromatography (MS–GC). Results compare favorably with a simple kinetic model. A Gaussian model overpredicts the concentration of larger rings. We believe this is the first study to actually measure rings in a nonequilibrium polymerization.

Introduction

Cyclization during stepwise polymerization is an old but still incompletely understood problem. Clearly there is a finite probability for two ends of the same chain to couple forming a closed circuit or ring. It is known qualitatively that increasing dilution, decreasing monomer molecular weight, and running the polymerization at stoichiometric balance all tend to increase the number of rings.[1,2] However, the dependence of cyclization on these variables has not yet been well quantified.

The problem is lack of accurate experimental measures of ring formation. Typically ring concentration is inferred from number-average molecular weight data. The difference between $\bar{M}_n$, the number of chain ends found by titration, and $\bar{M}_n$, that found by osmometry or other methods, is attributed to cyclic polymer. Errors in each of the techniques lead to rather large uncertainties in the number of rings. Furthermore, this method does not distinguish different ring sizes. Small amounts of side reaction will also be interpreted as ring formation. The problem is illustrated in Table I.

The $\bar{M}_n$ values were obtained by gel permeation chromatography (GPC) for a number of polymerized linear poly(dimethylsiloxane) (PDMS) systems studied in this work. The extent of reaction of one of the functional groups, p_A, was determined by titration and $\bar{M}_n$ was calculated by using a recursive method.[3] The ratio of moles of A groups to moles of B groups is called the reactant ratio, r. The samples were reacted in a diluted media at various concentrations, e.g., a concentration of 0.50 is 50% reactants and 50% dilution material. The column % R gives the range, accounting for various errors in each experimental determination, of the amount of rings formed in the system. This percentage of rings is calculated using Stepto's approach.[2]

In this paper we measure the rate of ring production directly on a PDMS system. Various analytical techniques are employed to quantify various ring sizes and amounts. The results from this study can be used in understanding cyclization as an effect on the gel point in nonlinear polymerizations.

Theory of Ring Formation

Linear condensation of two bifunctional monomers can be represented as follows:

$$\text{A–A} + \text{B–B} \rightarrow \text{A–(AB)}_{x-1}\text{–B} \qquad (1)$$

Table I
Determination of the Number of Rings from $\bar{M}_n$ for a Linear PDMS System

r	concn	$\bar{M}_n$[a]	P_A	$\bar{M}_n$[b]	% R[c]
0.9	1.00	1577 ± 150	0.956 ± 0.028	1724 ± 170	5–15
0.9	0.50	1310 ± 130	0.927 ± 0.027	1421 ± 140	8–18
0.9	0.10	790 ± 80	0.890 ± 0.026	1034 ± 100	15–25
0.7	1.00	666 ± 60	0.950 ± 0.028	757 ± 75	5–15
0.7	0.50	552 ± 50	0.905 ± 0.027	650 ± 65	8–18
0.7	0.10	441 ± 40	0.838 ± 0.025	532 ± 50	12–25

[a] By gel permeation chromatography (GPC). [b] Calculated from titration data. [c] Range.

where A and B are reactive groups and x is the number of monomer units (segments) in the molecule. If cyclization occurs in the polymerization, deviations from (1) result in

$$\text{A–A} + \text{B–B} \rightarrow \overbrace{\text{A–(AB)}_{y-1}\text{–B}} \qquad (2)$$

Jacobson and Stockmayer[1] developed a ring distribution function to account for cyclics in equilibrium linear condensations with the aid of configurational theory of randomly coiled chains. Flory has extended their theory to include the ring distributions in the condensation of the two bifunctional mnomers.[4] Linear systems at equilibrium can be solved exactly, but for systems in which there are no bond-breaking reactions, the solution becomes more involved. The introduction of time dependence leads to mathematical difficulties.

For linear chains, Gordon and Temple[5] have shown that the system of forward rate equations can be written down and solved numerically, in principle, to any desired degree of accuracy. These results can be compared with Flory's distribution at any given extent of reaction. Ring formation can also be included in the system of rate equations.

In a copolymerization, two bifunctional monomers react to form an alternating copolymer. The initial stages of the reaction are

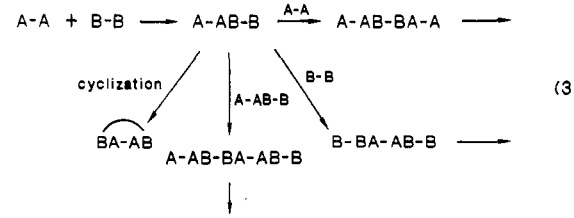

(3)

Assuming second-order kinetics, random flight statistics, and equal reactivity of all functional groups, a kinetic scheme can be written to describe the system.

The molecular species present in the reaction mixture can be divided into the following types: A_i = A–A(B–BA–A)$_{i-1}$ = chain terminating with type A functionalities;

† From: Rolando, R. J. M.S. Thesis, University of Minnesota, 1982; portions presented at IUPAC, Amherst, MA, 1982.

‡ Present address: Corporate Research, Process Technologies Laboratory, 3M, Bldg. 208-1-01, St. Paul, MN 55144.

0024-9297/87/2220-2707$01.50/0

Table II
System Reactants and Properties

model	compd	structure	form wt	purity by GC
B_2	1,3-divinyltetramethyldisiloxane	$CH_2{=}CHSiMe_2OSiMe_2CH{=}CH_2$	186.4	99.5%
$A_{2,2}$	tetramethyldisiloxane	$HSiMe_2OSiMe_2H$	134.3	99.0%
$A_{2,3}$	hexamethyltrisiloxane	$HSiMe_2OSiMe_2OSiMe_2H$	208.5	96.2%
$A_{2,4}$	1,1,3,3,5,5,7,7-octamethyltetrasiloxane	$HSiMe_2OSiMe_2OSiMe_2OSiMe_2H$	282.7	88.0%
catalyst[8]	*cis*-(dichloro)bis(diethyl sulfide)platinum(II)	$(C_2H_5)_2SPtCl_2S(C_2H_5)_2$	445	

B_i = B–B(A–AB–B)$_{i-1}$ = chain terminating with type B functionalities; M_i = (A–AB–B)$_i$ = chain with an even number of monomer units; R_i = $\overline{\text{(A–AB–B)}_i}$ = ring molecule. The species balances are as follows:

$$\frac{dA_i}{dt} = -2kA_i[2\sum_{j=1} B_j + \sum_{j=1} M_j] + 2k\sum_{j=1}^{i-1} M_j A_{i-j} \quad (4)$$

$$\frac{dB_i}{dt} = -2kB_i[2\sum_{j=1} A_j + \sum_{j=1} M_j] + 2k\sum_{j=1}^{i-1} M_j B_{i-j} \quad (5)$$

$$\frac{dM_i}{dt} = -2kM_i[\sum_{j=1} A_j + \sum_{j=1} B_j + \sum_{j=1} M_j] - k_c\frac{M_i}{f(i)} + k\left[4\sum_{j=1}^{i} A_j B_{i-(j+1)} + \begin{cases} 2\sum_{j=1}^{(i-1)/2} M_j M_{i-j} & i = \text{odd} \\ 2\sum_{j=1}^{(i-2)/2} M_j M_{i-j} + M_{i/2}^2 & i = \text{even} \end{cases}\right] \quad (6)$$

$$\frac{dR_i}{dt} = k_c\frac{M_i}{f(i)} \quad (7)$$

where k is the reaction rate constant for the linear step-growth reaction and k_c is the cyclization rate constant. Ring formation is a unimolecular reaction and each ring size is proportional to the concentration of the M_i from which it is formed. If the distribution of ring sizes is assumed to be Gaussian, then $f(i)$ can be approximated by $(iv)^{3/2}$. Here v is the number of bonds in the smallest ring that can be formed. This factor accounts for the decreased probability of forming large rings. However, real chemical systems are not this simple. Ring cyclization rates also depend on the (a) reactive species, (b) substituents in the ring, and (c) ring size itself.

Equations 4–7 can be solved numerically and the distribution of species can be known at any given time. Kinetic experimental results can be fitted and compared with the solution to the set of equations and values for k, k_c, and $f(i)$ can be measured. A goal of this work is to find $f(i)$, the ring size distribution function.

Experimental Section

Materials. The polydimethylsiloxane system used in this study is an end-linking reaction involving a hydrosilation between the silane hydrogen of one monomer and the vinyl end groups of the other:

$$SiH + CH_2{=}CH \xrightarrow{Pt} SiCH_2CH_2 \quad (8)$$

This reaction proceeds at room temperature with suitable catalyst concentration. Chalk and Harrod describe the reaction mechanism for this platinum-catalyzed reaction.[6] Hickey[7] has also discovered the possibility of a side reaction among the silane groups. Kinetic studies of this reaction support his theory.

In order to satisfy the optimum conditions for forming cyclics, small reactants were chosen to enhance ring formation. A vinyl end-capped PDMS, 1,3-divinyltetramethyldisiloxane (designated B_2), was obtained from the Dow Corning Corporation as one reactant. A series of three linear Si–H siloxanes were used to react with the B_2. They are tetramethyldisiloxane ($A_{2,2}$), hexamethyltrisiloxane ($A_{2,3}$) and 1,1,3,3,5,5,7,7-octamethyltetrasiloxane ($A_{2,4}$). These were obtained from Petrarch Systems Inc. Table II presents these chemical compounds along with other property information. In the notation used, the first subscript indicates functionality and the second subscript denotes monomer type.

Table III
Cyclic Sizes for Given Reactive System Number of Skeletal Atoms

reactant	ring of order 1	model designation	ring of order 2	model designation
$A_{2,2}$	10	$R_{1,10}$	20	$R_{2,20}$
$A_{2,3}$	12	$R_{1,12}$	24	$R_{2,24}$
$A_{2,4}$	14	$R_{1,14}$	28	$R_{2,28}$

Each reactant was analyzed for purity on a Hewlett-Packard Model 5730 gas chromatograph by thermal conductivity. This analysis used high-performance columns packed with 10% silicone oil (UCW-982) on a diatomaceous silica support (WAW-DMCS 80-100).

Ring Size. In the reaction of B_2 with $A_{2,2}$, the first ring structure that may form is the following:

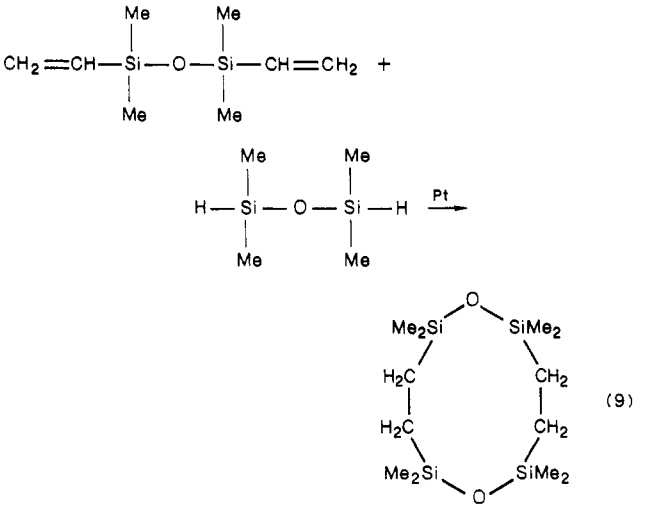

(9)

If each Si–O, C–C, and C–Si unit is counted as one repeat unit, then the ring that could form is v = 10, i.e., a molecule containing ten skeletal atoms. Similarly for the reaction of B_2 with $A_{2,3}$ or $A_{2,4}$. The first ring structure of each of these would be v = 12 and v = 14, respectively.

For the second-order ring structure that could form, v = 20, 24, and 28 for $A_{2,2}$, $A_{2,3}$, and $A_{2,4}$, respectively. Table III summarizes these results.

Procedures. Various reactant ratios (r = number of moles of A/number of moles of B) were reacted at room temperature in sealed vials for 72 h. The reaction between the silane hydrogen and the vinyl end groups is catalyzed by the platinum(II) complex shown in Table II. This catalyst was prepared by the reaction of potassium tetrachloroplatinate with an excess of diethyl sulfide[8] and then was dissolved in glass distilled toluene to about 1.0 wt %.

In order to enhance the possibility of loop formation, each r was reacted at various diluted concentrations. Glass-distilled toluene was used as a diluent because of PDMS solubility and toluene solutions can be used directly in several analytical techniques. Catalyst concentration was maintained at one drop catalyst for every milliliter of mixture.

To each reaction, approximately 3.0 wt % of cyclohexane is added to act as an internal standard for later analysis by gas

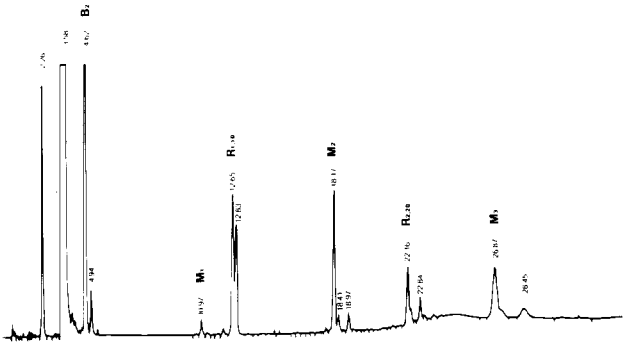

Figure 1. Typical gas chromatogram for the $A_{2,2} + B_2$ system.

Table IV
Mass Spectroscopy Results for the System $A_{2,2} + B_2$

peak retention time	mass no. (Dow)	mass no. (U of M)	peak retention time	mass no. (Dow)	mass no. (U of M)
2.26		84	18.17	507	506
3.58	78	78	18.90	507	506
4.62	186	186	22.16	640	640
10.97	320	320	22.84	640	640
12.65	320	320	26.87	827	827
12.83	320	320	28.45	827	827

chromatography. For $A_{2,2}$, r = 0.3, 0.5, 0.7, 0.8, 0.9, and 0.95; for $A_{2,3}$ and $A_{2,4}$, r = 0.7, 0.8, 0.9, and 0.95, for each r value concentrations of toluene at 9, 25, 50, 80, and 90 vol % were used. These reactions were run to completion.

Gas chromatography was used to study each reacted system. A Hewlett-Packard Model 5840A gas chromatograph equipped with a flame ionization detector (FID) and a 35-sample automatic injection system was used. Because of the long retention times (approximately 50 min) encountered in this study, the automatic sampler aided in data acquisition tremendously. Nitrogen was used as a carrier gas with a flow of approximately 25 mL/min. Air (approximately 300 mL/min) and hydrogen (approximately 25 mL/min) provide the best conditions for analysis by this instrument by keeping both flame intensity and response consistent.

The FID becomes extremely important because of the wide temperature range employed to analyze a given reaction mixture. Each silicone sample was run on temperature program from 70 to 300 °C at a rate of 10 °C/min. At 300 °C, analysis is continued for approximately 30 min, making the total run approximately 50 min. This change in the temperature program causes some change in the flow rate of the carrier gas, but FID response is not affected by such changes. Figure 1 shows a typical chromatogram for the $B_2 + A_{2,2}$ polymerization, where an excess of B_2 was used.

Mass spectroscopy–gas chromatography (MS–GC) was done on a representative sample of the $A_{2,2} + B_2$ system. The sample was analyzed by the Dow Corning Corporation and by the Mass Spectroscopy Lab at the University of Minnesota and mass numbers were obtained for various peaks. Both analyses revealed more than one peak with the same mass number. Table IV lists the various results. In the table some of mass numbers are corrected because of the probable loss of a methyl group (15 mass units) which is common for those molecules.[9]

Nuclear magnetic resonance was done on the components at GC peaks 12.65 and 12.83 (mass number 320; see Figure 1). It was found that two cyclic structures were formed. One was the expected 10-atom ring, $R_{1,10}$, but the other was a nine-membered ring, $R_{1,9}$. This analysis revealed that reaction could occur on the α-carbon of the vinyl end group in addition to the preferred β-addition reaction. This would account for the appearance of more than one peak of the same mass number. These results are discussed in a separate paper.[10] The α-addition was also shown to occur by Andrinov and co-workers.[11] Table V summarizes the proposed structures for each system based on the above results. In the remainder of this paper designation of $R_{1,10}$ combines both the $R_{1,9}$ and $R_{1,10}$ structures. All the results presented combine the various peaks with the same mass numbers which correspond to a given structure.

Table V
Proposed Structures

system	peak designation	form wt	proposed struct
$A_{2,2} + B_2$	$R_{1,10}$	320.7	-A-AB-B-
	M_1	320.7	A-AB-B
	B_2	507.1	B-BA-AB-B
	$R_{2,20}$	641.4	-(A-AB-B)$_2$-
	B_3	827.8	B-B(A-AB-B)$_2$
	A_2	455.0	A-AB-BA-A
	A_3	775.7	A-A(B-BA-A)$_2$
$A_{2,3} + B_2$	$R_{1,12}$	394.9	-A-AB-B-
	B_2	581.3	B-BA-AB-A
	$R_{2,24}$	789.8	-(A-AB-B)$_2$-
	B_3	976.2	B-B(A-AB-B)$_2$
$A_{2,4} + B_2$	$R_{1,14}$	469.1	-A-AB-B-
	B_2	655.5	B-BA-AB-A
	$R_{2,28}$	938.2	-(A-AB-B)$_2$-
	B_3	1124.6	B-B(A-AB-B)$_2$

Table VI
Correlation Study Compounds

designation	$\bar{M}_n$	no. of Me	structure
B_2	186.4	4	$CH_2{=}CHSiMe_2OSiMe_2CH{=}CH_2$
$A_{2,2}$	134.3	4	$HSiMe_2OSiMe_2H$
$A_{2,3}$	208.5	6	$HSiMe_2OSiMe_2OSiMe_2H$
$A_{2,4}$	282.7	8	$HSiMe_2OSiMe_2OSiMe_2OSiMe_2H$
C_2	162.4	6	$MeSiMe_2OSiMe_3$
C_3	236.6	8	$MeSiMe_2OSiMe_2OSiMe_3$
C_4	310.7	10	$MeSiMe_2OSiMe_2OSiMe_2OSiMe_3$
D_4	296.6	8	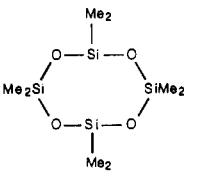

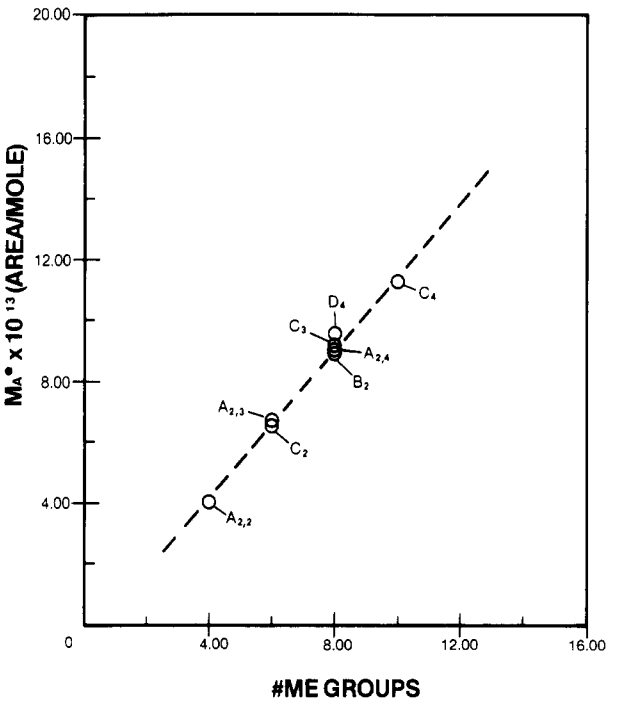

Figure 2. Methyl group/concentration calibration curve.

In order to interpret concentration from GC peak areas, a calibration based the number of methyl group on a given molecule was developed. Table VI lists the compounds used to determine the detector response per methyl group. Figure 2 has the actual calibration data plotted as peak area response/mole (defined as M^*_A) versus the number of methyl groups. It was deduced that

one vinyl group was equivalent to two methyl groups. Table VII summarizes the results of this calibration when applied to each system studied. This allows for direct determination of product concentrations.

The reaction extent was determined by measuring the amount of vinyl groups remaining at the end of the reaction by titrating for the excess vinyl groups using a procedure outlined by Smith (ref 12, p 152). The unsaturated vinyl groups react with saturated mercuric acetate in methanol to produce 1 equiv of acetic acid for each double bond. Errors are consistently less than 2% which make this a reproducible measurement. Number-average molecular weights, $\bar{M}_n$, in Table I were determined by gel permeation chromatography (GPC) using a Varian Model 5000 liquid chromatograph containing six Waters μ-Styrogel columns and analyzed by a Micrometrics 771 refractive index detector. This work was done at the 3M in St. Paul, MN. The predicted values of $\bar{M}_n$ were calculated from r and p by using an extension of the recursive method described by Macosko and Miller.[13] Note that the recursive method does not account for intramolecular reaction.

Results

The polymerization rate constant was determined by evaluating the initial rate of appearance of the first possible species to be formed, i.e., M_1. Equation 6 for $i = 1$ is used to calculate k:

$$dM_1/dt = kA_1B_1 \quad (10)$$

The concentrations of species A_1, B_1, M_1, and $R_{1,10}$ were measured at various times for $r = 0.5$ and 0.95. The rate constant, k, was found to be 3.1×10^{-4} L (mol min)$^{-1}$ for this approximation.

Rate balances can be written on the individual species A_1, B_1, M_1, and R_1 and on the total polymer distributions of each type of molecule, i.e., $\sum_i A_i$, $\sum_i B_i$, $\sum_i M_i$, and $\sum_i R_i$. It was found experimentally that most of the rings are either R_1 or R_2, the total ring distribution can be approximated by $\sum_i R_i \cong R_1 + R_2$. As shown earlier, only the first few species can be measured by GC.

The system of equations can be written as follows:

$$dA_1/dt = -2kA_1(2B + M) \quad (11)$$

$$dB_1/dt = -2kB_1(2A + M) \quad (12)$$

$$dM_1/dt = 4kA_1B_1 - 2kM_1(A + B + M) - k_{c1}M_1 \quad (13)$$

$$dA/dt = -4kAB \quad (14)$$

$$dB/dt = -4kAB \quad (15)$$

$$dM/dt = -2kM(A + B) + 4kAB - k_{c1}M_1 - k_{c2}M_2 \quad (16)$$

$$dA_2/dt = -2kA_2(2B + M) + 2kM_1A_1 \quad (17)$$

$$dB_2/dt = 2kB_2(2B + M) + 2kM_1B_1 \quad (18)$$

$$dM_2/dt = 4kA_2B_1 + 4kB_2A_1 - 2kM_2(A + B + M) + kM_2M_2 - k_{c2}M_2 \quad (19)$$

$$dR_1/dt = k_{c1}M_1 \quad (20)$$

$$dR_2/dt = k_{c2}M_2 \quad (21)$$

$$dR/dt = k_{c1}M_1 + k_{c2}M_2 \quad (22)$$

where $k = 3.1 \times 10^{-4}$ L (mol min)$^{-1}$, $k_{c1} = k_c/f(1)$, $k_{c2} = k_c/f(2)$, $A = \sum_i A_i$, $B = \sum_i B_i$, $M = \sum_i M_i$, and $R = \sum_i R_i$. For a Gaussian distribution of ring sizes, $f(i) = (iv)^{3/2}$ for $v = 10$, $f(1) = 0.0316$, and $f(2) = 0.0112$. Equations 11–22 were solved numerically by a Runga–Kutta routine using the experimentally determined k and optimizing for k_c (using the Gaussian assumption) by fitting the final data ($t = \infty$ reaction complete, i.e., high p) for each species at the various r's. This was done by incrementing k_c until a "fitted" solution was obtained. This method produced a $k_c = 1.6 \times 10^{-3}$ L (mol min)$^{-1}$ which best fit the final data.

Table VII
Calculated M^*[a] for Proposed Structures

system	peak designation	$\bar{M}_n$	equiv Me groups[a]	$M_A^* \times 10^{-13}$, area/mol
$A_{2,2} + B_2$	M_1	320.7	10	11.51
	$R_{1,10}$	320.7	8	9.08
	M_2	507.1	16	18.81
	$R_{2,20}$	641.4	16	18.81
	M_3	827.8	24	28.54
	M_2^*	455.0	12	13.94
	M_3^*	775.7	20	23.67
$A_{2,3} + B_2$	$R_{1,12}$	394.9	10	11.51
	M_2	581.3	18	21.24
	$R_{2,24}$	789.8	20	23.67
	M_3	976.2	28	33.39
$A_{2,4} + B_2$	$R_{1,14}$	469.1	12	13.94
	M_2	655.5	20	24.32
	$R_{2,28}$	938.2	24	28.54
	M_3	1124.6	32	38.26

[a] Equivalent methyl groups = no. Me groups + 2(no. C=C groups).

Table VIII
Experimental vs Calculated $[R_1]$ in the Bulk

r	p (from titration)	$[R_1]_{exptl} \times 10^2$, mol/L	$[R_1]_{calcd} \times 10^2$, mol/L
0.5	0.908	3.42	3.30
0.7	0.950	4.92	4.90
0.8	0.952	5.61	5.40
0.9	0.956	5.58	5.75
0.95	0.963	5.98	6.10

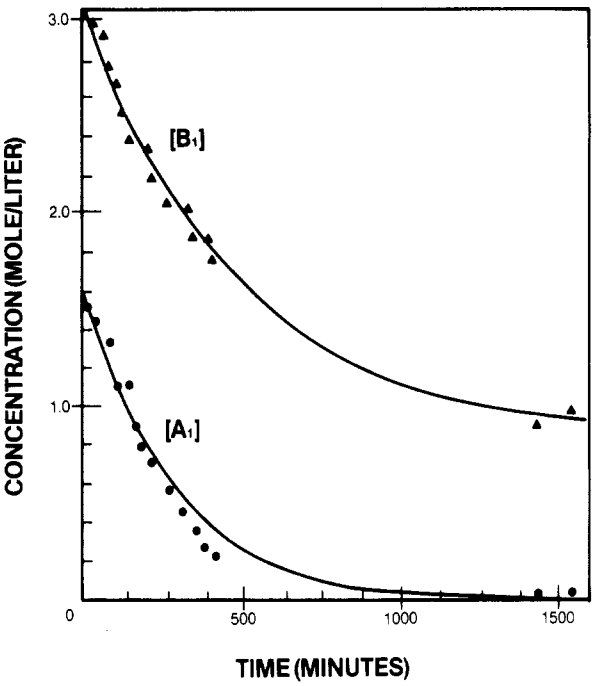

Figure 3. Experimental vs "fitted" results for the monomer disappearance at $r = 0.5$ and $k_c = 1.6 \times 10^{-3}$ L (mol min)$^{-1}$.

Figures 3–8 present the experimental versus calculated results for each species at $r = 0.5$ and 0.95. The general trend of the data being below the fitted curve could be explained by a possible side reaction of the silane hydrogen.

Equations 11–22 can be solved for concentrations of a given species as a function of reaction extent, p, because p is a function of time. For a given p, the concentration of a specific species can be determined at a certain r. Table VIII shows the influence of r on the amount of $R_{1,10}$ formed. The experimental values were determined by gas chro-

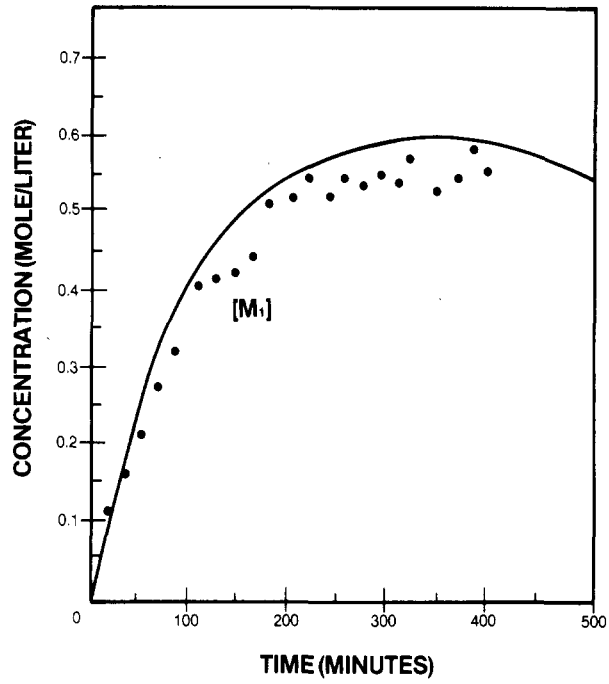

Figure 4. Experimental vs "fitted" results for the dimer (A-AB-B) concentration, $[M]$, at $r = 0.5$ and $k_c = 1.60 \times 10^{-3}$ L (mol min)$^{-1}$.

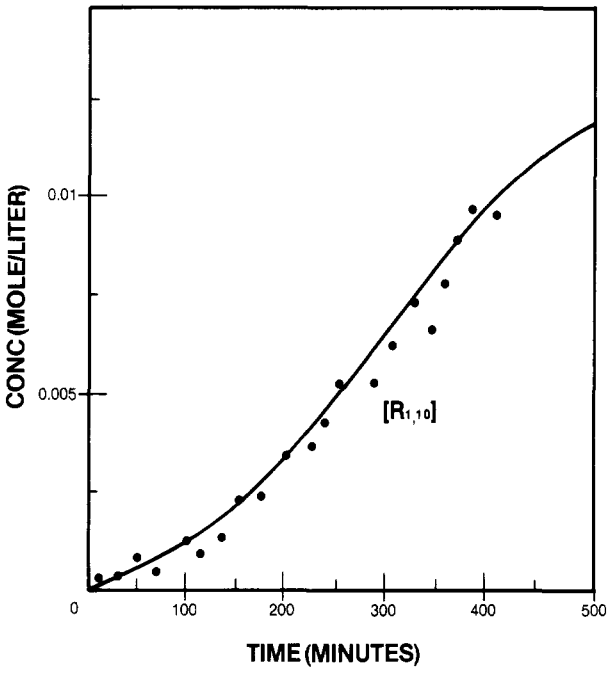

Figure 5. Experimental vs "fitted" results for the cyclic (A-AB-B) concentration, $[R_{1,10}]$, at $r = 0.5$ and $k_c = 1.60 \times 10^{-3}$ L (mol min)$^{-1}$.

matography and by using the methyl group correlation. The concentration of $R_{1,10}$ increases as r approaches unity. Table IX demonstrates the effect of diluent on ring formation. $R_{1,10}$ increases with increasing dilution. Figure 9 shows $[R_{1,10}]$ as function of both r and dilution.

The amounts of $R_{1,12}$, $R_{1,14}$, $R_{2,20}$ $R_{2,24}$, and $R_{2,28}$ were also measured at the same r's and p's as $R_{1,10}$. Table X compares the ratios of these ring sizes to $R_{1,10}$ in the bulk reactions.

The ratio then of $R_{1,10}$:$R_{1,12}$:$R_{1,14}$:$R_{2,20}$:$R_{2,24}$:$R_{2,28}$ is 1:0.80:0.75:0.20:0.06:0.06. This says that in bulk solution of equivalent numbers of reactive groups (r the same) that $R_{1,10}$ and $R_{2,20}$ would form more than the other pair. Re-

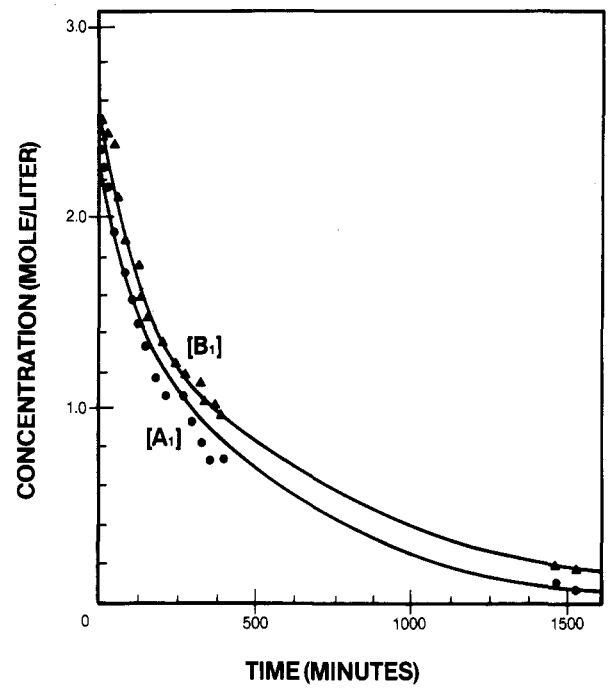

Figure 6. Experimental vs "fitted" results for the monomer disappearance at $r = 0.95$ and $k_c = 1.6 \times 10^{-3}$ L (mol min)$^{-1}$.

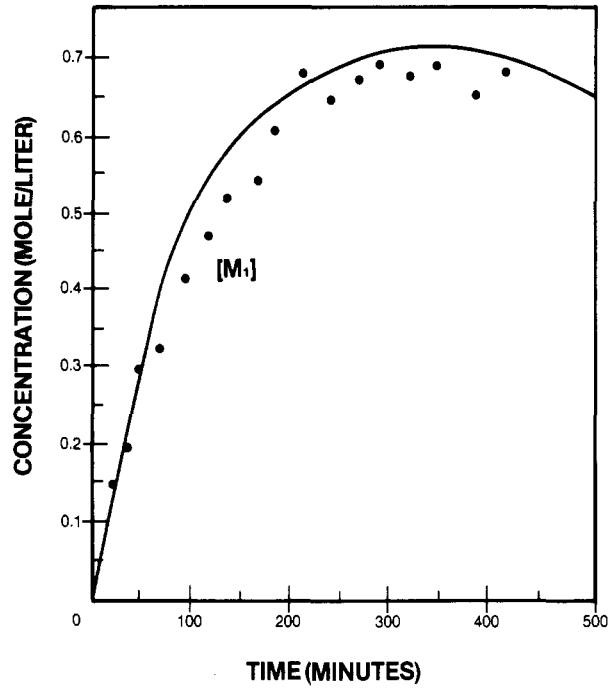

Figure 7. Experimental vs "fitted" results for the dimer (A-AB-B) concentration, $[M_1]$, at $r = 0.95$ and $k_c = 1.6 \times 10^{-3}$ L (mol min)$^{-1}$.

Table IX
Experimental vs Calculated $[R_1]$ in Dilution

r	concn	p (from titration)	$[R_1]_{exptl} \times 10^2$, mol/L	$[R_1]_{calcd} \times 10^2$, mol/L
0.9	1.0	0.956	5.6	5.8
0.9	0.5	0.927	8.8	9.2
0.9	0.7	0.915	13.2	13.6
0.9	0.1	0.890	14.8	13.8
0.7	1.0	0.950	4.9	4.9
0.7	0.5	0.905	7.8	8.4
0.7	0.2	0.872	12.3	12.8
0.7	0.1	0.838	13.3	13.5

member $R_{1,12}$ and $R_{1,14}$ are the first rings that can form in the $A_{2,3}$ and $A_{2,4}$ systems, respectively. They are also the

Table X
Ratios of Ring Sizes

sample	$R_{1,10}/R_{1,10}$	$R_{1,12}/R_{1,10}$	$R_{1,14}/R_{1,10}$	$R_{2,20}/R_{1,10}$	$R_{2,24}/R_{1,10}$	$R_{2,28}/R_{1,10}$
0.7 (100)	1	0.80	0.70	0.19	0.06	0.05
0.8 (100)	1	0.72	0.65	0.20	0.05	0.05
0.9 (100)	1	0.86	0.79	0.21	0.06	0.06
0.95 (100)	1	0.82	0.79	0.22	0.06	0.08
		av 0.84 ± 0.05	av 0.75 ± 0.6	av 0.20 ± 0.01	av 0.06 ± 0.1	av 0.06 ± 0.01
exptd Gaussian ratio	1	0.76	0.60	0.35	0.27	0.21

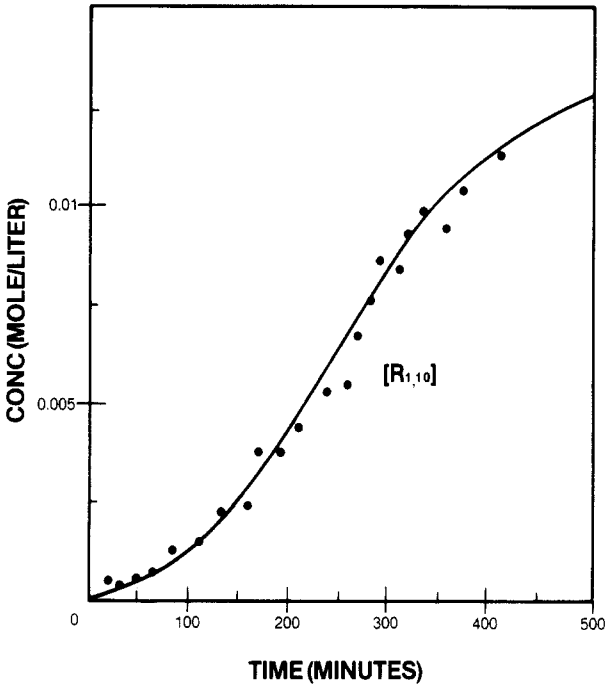

Figure 8. Experimental vs "fitted" results for the cyclic (A–AB–B) concentration, $[R_{1,10}]$, at $r = 0.95$ and $k_c = 1.6 \times 10^{-3}$ L (mol min)$^{-1}$.

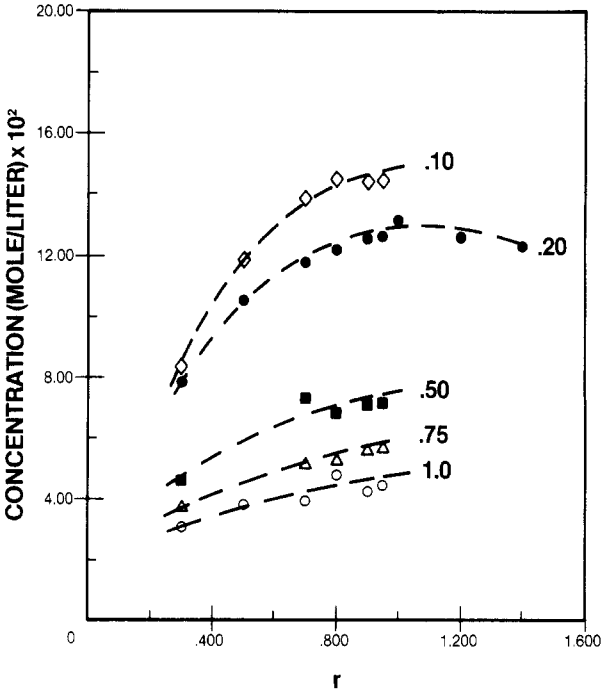

Figure 9. $[R_{1,10}]$ as a function of r and dilution.

total of the proposed α- and β-addition reactions.

If the formation of these rings follows a Gaussian distribution, then the ring-forming rate constants, $k_{ci} = k_c/(iv)^{3/2}$, for each R_i are directly related to the ring concentrations. However, for these three systems, Table X shows deviation from the Gaussian assumption using $k_c = 1.6 \times 10^{-3}$ L (mol min)$^{-1}$. The R_1 rings form more rapidly than the Gaussian prediction and R_2 more slowly. In order to test this more directly, reaction rate constants for the $A_{2,3}$ and $A_{2,4}$ systems must be measured in order to predict final species concentrations. The formation of the R_1's is more dependent on other factors such as catalyst size and the existence of other substituent groups on the molecule. These factors would give a better indication of the ring distribution function, i.e., $f(i)$, for a given system. The Gaussian model will apply only at larger ring sizes, and for these systems, it is not useful.

Conclusions

The major goal of this study of linear polymerization in a selected silicone system was to identify and quantify small cyclics. Rings of order one and two were calculated by using a kinetic model and measured experimentally. We believe this is the first study to actually measure rings in a nonequilibrium polymerization.

Production of rings was found to be a maximum at $r = 1$ if no side reaction occurs. Rings of smaller size will form in more abundance than larger rings. But for our chemical system Gaussian statistics overpredict the concentration of larger rings. Ring formation in linear systems can be important, especially with dilution, and failure to realize this could lead to undesirable results.

Guidelines have been established to further study these systems. Specific techniques were used in this investigation in an effort to identify cyclics. Gas chromatography is an excellent method to separate and quantify rings, especially when combined with mass spectroscopy and NMR. Problems occur in relating detector response to molecular structure.

Determination of $\bar{M}_n$ by GPC is vulnerable to errors and leads to no specific conclusions about using $\bar{M}_n$ to calculate the amount of rings in a system. There is too much variability in the results. However, $\bar{M}_n$ determined experimentally was less than that predicted which would be expected in a ring-forming system.

The PDMS system used seems to satisfy the requirements for this problem. Rings with skeletal atoms of 10, 12, and 14 form in significant amounts (3–4% in bulk). This aids in their detection and study. Possible side reactions kept $p < 1$ for the polymerization portion of the reaction. The isomers formed by addition to the α-carbon are shown by the data. The approach used in this study can be extended to nonlinear polymerization. Some preliminary experimental results have been obtained.[14]

Acknowledgment. Special thanks are given to the Army Research Office for funding this work, Doug Miller of George Washington University for aid in theoretical aspects, and 3M and Dow Corning for some analytical results.

Registry No. B_2, 2627-95-4; $A_{2,2}$, 3277-26-7; $A_{2,3}$, 1189-93-1; $A_{2,4}$, 1000-05-1; $R_{1,10}$, 110271-15-3; $R_{1,12}$, 110271-16-4; $R_{1,14}$, 110271-17-5; $R_{2,20}$, 110271-18-6; $R_{2,24}$, 110271-19-7; $R_{2,28}$, 110271-20-0; $(A_{2,2})(B_2)$ (copolymer), 68015-65-6; $(A_{2,2})(B_2)$ (SRU),

110294-68-3; $(A_{2,3})(B_2)$ (copolymer), 87318-28-3; $(A_{2,3})(B_2)$ (SRU), 110294-69-4; $(A_{2,4})(B_2)$ (copolymer), 87318-29-4; $(A_{2,4})(B_2)$ (SRU), 110294-70-7.

References and Notes

(1) Jacobson, H.; Stockmayer, W. H. *J. Chem. Phys.* **1950**, *18*, 1600.
(2) Stepto, R.; Waywell, D. *Makromol. Chem.* **1972**, *152*, 263.
(3) Lopez-Serrano, F.; Castro, J. M.; Macosko, C. W.; Tirrell, M. *Polymer* **1980**, *21*, 263.
(4) Flory, P. J. *Principles of Polymer Chemistry*; Cornell University Press: Ithaca, NY, 1953.
(5) Gordon, M.; Temple, W. B. *Makromol. Chem.* **1972**, *152*, 277.
(6) Chalk, A. J.; Harrod, J. F. *J. Am. Chem. Soc.* **1965**, *87*, 16.
(7) Hickey, W. J. M.S. Thesis, University of Minnesota, 1980.
(8) Kauffman, C. B.; Cowan, D. O. In *Inorganic Synthesis*; Rochow, E. G., Ed.; McGraw-Hill: New York, 1969; Vol. 6, p 214.
(9) Hill, H. C. *Introduction to Mass Spectroscopy*; Heyden and Son: New York, 1972.
(10) Rolando, R. J.; Fristad, manuscript in preparation.
(11) Andrinov, K. A.; Souchek, I.; Getfleisch, I.; Khananashvilli, L. M. *Izv. Akad. Nauk SSSR, Ser. Khim.* **1975**, *4*, 965.
(12) Smith, A. *Analysis of Silicones*; Wiley: New York, 1974.
(13) Macosko, C. W.; Miller, D. R. *Macromolecules* **1976**, *9*, 199.
(14) Rolando, R. J. M.S. Thesis, University of Minnesota, 1982.

Physical Cross-Linking of Mesomorphic Polymers Containing Spiropyran Groups†

Ivan Cabrera and Valeri Krongauz*

Department of Structural Chemistry, The Weizmann Institute of Science, Rehovot 76100, Israel.

Received February 20, 1987

ABSTRACT: Acrylic copolymers with mesogenic and spiropyran side chains give a mesophase, which on heating is converted to an isotropic melt, displaying strong dynamic birefringence. This effect is connected with the thermochromic spiropyran–merocyanine transformation resulting in the physical cross-linking of the macromolecules due to merocyanine aggregation.

Earlier, we reported[1,2] a new type of crystallization of atactic vinyl polymers bearing spiropyran side groups, by swelling in polar solvents. Solvatochromic spiropyran–merocyanine conversion and self-assembly of merocyanine groups into giant molecular stacks are the driving forces for this crystallization.

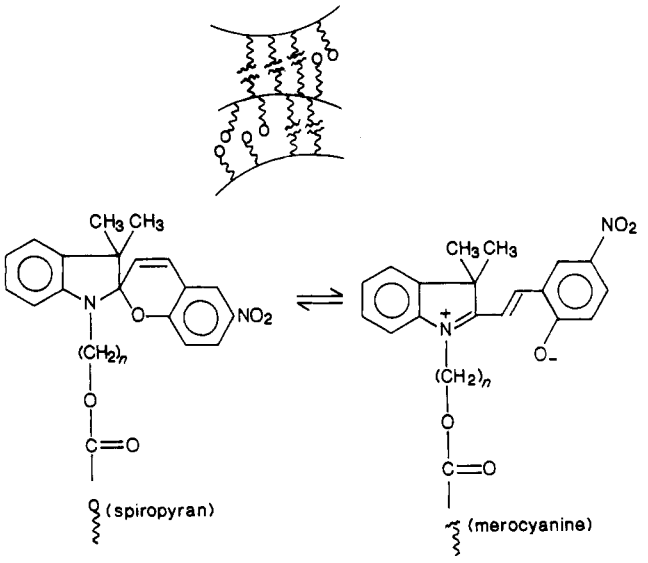

We believe that the high degree of crystallinity of the above polymers (up to 40%) was achieved because the cooperative spiropyran–merocyanine conversion occurs step-by-step along the polymer chains, a process which we called "zipper crystallization". The tendency of the merocyanine groups to self-assembly is so strong that even in a 1:1 copolymer of a spiropyran methacrylate with methyl methacrylate it proceeds rather fast, though it does not result in crystalline order.[3]

The assumed structure of the assemblies resembles the structure of side chain liquid crystal polymers, though the factors that give rise to these structures are completely different: the merocyanine stacks, formed in the course of swelling, belong to the so-called H-type, which is characterized by antiparallel dipole–dipole interactions of the molecules.[4] The liquid crystalline structure, on the other hand, is determined mainly by the steric factor connected with the geometrical anisotropy of the mesogenic groups.[5]

Recently, we have shown that the combination of thermochromic spiropyran and mesogenic groups in a low molecular weight molecule gives a new kind of mesophase, quasi-liquid crystals.[6,7]

One can expect that in copolymers containing both spiropyran and mesogenic side groups the competition between merocyanine interactions and liquid crystalline ordering of mesogenic groups will give rise to new, interesting structural changes of the mesophase, taking into account that spiropyran can be effectively converted into merocyanine both by light and by heat.

To test these expectations, and in order to make spiropyran groups more compatible with mesogenic ones, new spiropyran acrylate monomers

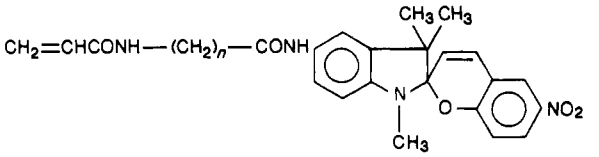

were now synthesized (Table I), in which the acrylic group is attached through a flexible spacer to the indoline part of the spiropyran. Copolymerization with an acrylic monomer containing a mesogenic group[8]

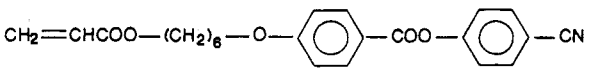

leads to liquid crystal copolymers with thermochromic properties. We now report structural transformations occurring in such copolymers: Physical cross-linking of the macromolecules due to aggregation of the dye moieties gives rise to formation of a network responsible for the

†Dedicated to Prof. Ernst Fischer on the occasion of his 65th birthday. His pioneering studies on spiropyrans inspired our long-lasting interest in these fascinating substances.

0024-9297/87/2220-2713$01.50/0